

AD-A099 321 ARMY MISSILE COMMAND REDSTONE ARSENAL AL SYSTEMS SI--ETC F/8 20/4
EFFECT OF FOREBODY WING STRAKES ON ENHANCING PERFORMANCE OF A T--ETC(U)
AUG 80 P K ALSTOTT, W D WASHINGTON SBIE-AD-E950 125 NL

UNCLASSIFIED

DRSHI/RD-80-13-TR

SBIE-AD-E950 125

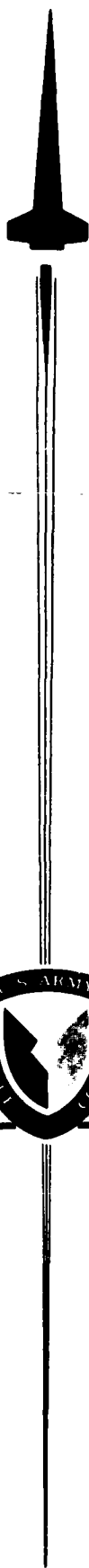
NL

1 of 1
2009.421

END
DATE
FILMED
8-81
DTIC

(12) LEVEL III — AD-E950125
43

AD A 099 321



TECHNICAL REPORT RD-80-13 ✓

EFFECT OF FOREBODY WING STRAKES ON
ENHANCING PERFORMANCE OF A TYPICAL
BODY-WING-TAIL MISSILE CONFIGURATION AT
MACH 2.0

Pamela K. Alstott
William D. Washington
Systems Simulation and Development Directorate
US Army Missile Laboratory

August 1980



U.S. ARMY MISSILE COMMAND

Redstone Arsenal, Alabama 35898

DTIC
ELECTE
MAY 20 1981
S D

B

DISTRIBUTION STATEMENT A

Approved for public release;
Distribution Unlimited

DTIC FILE COPY

FORM 1021, 1 JUL 79 PREVIOUS EDITION IS OBSOLETE

81 5 19 001

DISPOSITION INSTRUCTIONS

**DESTROY THIS REPORT WHEN IT IS NO LONGER NEEDED. DO NOT
RETURN IT TO THE ORIGINATOR.**

DISCLAIMER

**THE FINDINGS IN THIS REPORT ARE NOT TO BE CONSTRUED AS AN
OFFICIAL DEPARTMENT OF THE ARMY POSITION UNLESS SO DESIGNATED
BY OTHER AUTHORIZED DOCUMENTS.**

TRADE NAMES

**USE OF TRADE NAMES OR MANUFACTURERS IN THIS REPORT DOES
NOT CONSTITUTE AN OFFICIAL INDORSEMENT OR APPROVAL OF
THE USE OF SUCH COMMERCIAL HARDWARE OR SOFTWARE.**

UNCLASSIFIED

SECURITY CLASSIFICATION OF THIS PAGE (When Data Entered)

REPORT DOCUMENTATION PAGE		READ INSTRUCTIONS BEFORE COMPLETING FORM	
1. REPORT NUMBER TR-RD-80-13 ✓	2. GOVT ACCESSION NO. RD-A099	3. RECIPIENT'S CATALOG NUMBER 321	
4. TITLE (and Subtitle) EFFECT OF FOREBODY WING STRAKES ON ENHANCING PERFORMANCE OF A TYPICAL BODY-WING-TAIL MISSILE CONFIGURATION AT MACH 2.0	5. TYPE OF REPORT & PERIOD COVERED Technical Report		
	6. PERFORMING ORG. REPORT NUMBER		
7. AUTHOR(s) Pamela K. Alstott William D. Washington	8. CONTRACT OR GRANT NUMBER(s)		
9. PERFORMING ORGANIZATION NAME AND ADDRESS Commander, US Army Missile Command ATTN: DRSMI-RD Redstone Arsenal, AL 35898	10. PROGRAM ELEMENT, PROJECT, TASK AREA & WORK UNIT NUMBERS		
11. CONTROLLING OFFICE NAME AND ADDRESS Commander US Army Missile Command ATTN: DRSMI-RPT Redstone Arsenal, AL 35898	12. REPORT DATE August 1980		
	13. NUMBER OF PAGES 33		
14. MONITORING AGENCY NAME & ADDRESS (if different from Controlling Office)	15. SECURITY CLASS. (of this report) UNCLASSIFIED		
	15a. DECLASSIFICATION/DOWNGRADING SCHEDULE		
16. DISTRIBUTION STATEMENT (of this Report) APPROVED FOR PUBLIC RELEASE; DISTRIBUTION UNLIMITED.			
17. DISTRIBUTION STATEMENT (of the abstract entered in Block 20, if different from Report)			
18. SUPPLEMENTARY NOTES			
19. KEY WORDS (Continue on reverse side if necessary and identify by block number) Strakes Vortex High Angles of Attack			
20. ABSTRACT (Continue on reverse side if necessary and identify by block number) The addition of forebody strakes to aircraft configurations have shown significant improvement in aircraft performance at moderate-to-high angles-of-attack for subsonic and transonic speeds. This research project investigates the effect of strakes on missile type body-wing-tail configurations at supersonic speeds by conducting a (1) literature survey of related existing data and design methods and (2) analyzing a new set of wind tunnel data on a body-wing-tail missile configuration with added forebody strakes at Mach 2.0. Findings from the literature survey are presented. Analysis of the wind tunnel data			

DD FORM 1 JAN 73 1473 EDITION OF 1 NOV 68 IS OBSOLETE

UNCLASSIFIED

SECURITY CLASSIFICATION OF THIS PAGE (When Data Entered)

SECURITY CLASSIFICATION OF THIS PAGE(When Data Entered)

Block #20. (cont.)

reveals that added forebody strakes do not significantly improve missile performance at Mach 2.0 and angles-of-attack up to 20 degrees for the configuration tested.

SECURITY CLASSIFICATION OF THIS PAGE(When Data Entered)

CONTENTS

	Page No.
I. INTRODUCTION	4
II. LITERATURE SURVEY	4
A. Findings	
B. Strake Design	
III. EXPERIMENTAL DATA	5
A. Apparatus and Test	
B. Models and Data	
IV. RESULTS AND DISCUSSION	5
A. Wings	
B. Tail Fins	
V. CONCLUSIONS	6
REFERENCES	10
SURVEY BIBLIOGRAPHY	29
NOMENCLATURE	31

Accession For	
NTIS GRA&I	<input checked="" type="checkbox"/>
DTIC TAB	<input type="checkbox"/>
Unannounced	<input type="checkbox"/>
Justification_____	
By_____	
Distribution/_____	
Availability Codes	
	Avail and/or
Dist	Special
A	

LIST OF FIGURES

	Page No.
1. Definition of Effective Strake Area for a Simple Wing-Body Configuration .	11
2. Typical Configuration	11
3. Body-Tail Details	12
4. Strake Dimensions (Inches)	13
5. Strake Size Relative to Wing (W_1)	14
6. Flow Angularity ($M^\infty = 2$)	15
7. Flow Angularity ($M^\infty = 3$)	16
8. Effect of Strakes on Wing Plug Wing-Body Interference ($\theta = 0^\circ$)	17
9. Effect of Strakes on Wing Plus Wing-Body Interference ($\theta = 45^\circ$)	18
10. Normal Force Ratio (Wing With Strake/Wing Without Strake)	19
11. Fin Normal Force (All Fins)	20
12. Effect of Strake S_2 on Fin Normal Force	21
13. Effect of Strake S_2 on Fin Hinge Moment	22
14. Effect of Strake S_2 on Fin Root Bending Moment	23
15. Strake S_2 Effect on Fin Normal Force at $\theta = 45^\circ$	24
16. Effects of Strake S_2 on Total Configuration Stability ($\theta = 0^\circ$)	25
17. Effect of Strake S_2 on Total Configuration Stability ($\theta = 45^\circ$)	26
18. Ratio of Total Normal Force With and Without Strakes	27
19. Effect of Strake S_2 on Lift/ Drag Ratio	28
20. Effect of Mach Numbers on Lift/ Drag Ratio (No Strake)	28

LIST OF TABLES

	Page No.
1. Nominal Test Conditions	7
2. Body Geometry (B _i)	7
3. Strake Geometry (S _i)	8
4. Wing Geometry (W _i)	8
5. Tail Geometry (T _i)	9
6. Configuration Nomenclature	10

I. INTRODUCTION

The addition of forebody strakes to aircraft configurations has shown significant improvement in aircraft performance at moderate-to-high angles-of-attack for subsonic and transonic speeds. The principle reason for improvement is a significant increase in usable lift due to strake induced vortex effects on the basic wing lift. The strake leading edge vortex interacts with the boundary layer over the wing upper surface and, consequently, delays separation at high angles-of-attack. The delayed separation gives higher trim angles-of-attack and thus higher trim lift or maneuverability. Strake geometry is of secondary importance but still must be considered in design because of a possible adverse effect in pitch stability at high angles of attack. Several papers have documented forebody strake effects at subsonic and transonic speeds, but does this effect carry over to supersonic speeds?

This research project investigates the effect of strakes on missile type body-wing-tail configurations at supersonic speeds by (1) conducting a literature survey of existing data and design methods for strakes applicable to missile configurations and (2) analyzing a set of wind tunnel data obtained by MICOM on a body-wing-tail missile with strakes at Mach 2.0. The literature survey was accomplished using NASA and DOD computer search facilities plus any additional known references. Findings from the literature survey, as well as any strake design information, are presented. The experimental data used for Mach 2.0 analysis is part of a wind tunnel test conducted by MICOM at AEDC to study advanced interceptor missile configurations. The primary question to answer from this research is: Can strakes be used to improve high angle-of-attack performance of body-wing-tail missile configurations at supersonic speeds?

II. LITERATURE SURVEY

A literature survey was conducted to review articles and reports dealing with the effects of wing strakes on a body-wing-tail configuration's maneuverability. The literature was gathered by using a library search routine of both NASA and DOD material based on the key words, strake, and high angle-of-attack. Of the material reviewed,

approximately 90% dealt with aircraft wing-strake configurations rather than actual missile configurations. It is assumed that a missile wing-strake would respond in the same manner.

A. Findings

(1) Wing configurations that benefit most by the addition of the strake are those with low-to-moderate sweep angles ($<45^\circ$). Above 45° , the effects of strakes decrease corresponding to loss of interference lift. This occurs because wings having leading edge sweep angles greater than 45° develop high levels of vortex lift and, therefore do not require the additional vortex created by a strake (Survey Bibliography 13).

(2) Strakes were found to delay conventional stall by increasing maximum usable lift and decreasing lift-dependent drag at high incidences for subsonic and transonic speeds.

(3) For the transonic regions, strake addition yielded a decrease in buffet intensity.

(4) At supersonic Mach numbers, strake applications reduced wave drag and trimmed-induced drag.

(5) The combined effects of (1, 2, and 3) lead to a configuration that enhances the high angle-of-attack maneuver aerodynamics and does not, in doing so, detract from the low angle-of-attack ($<8^\circ-10^\circ$) portion of a mission.

(6) Increase in L/D ratios, due to lift increase at low speed and drag decrease at supersonic speed, was also a noticeable effect of strake addition.

B. Strake Design

In designing strakes, their performance is based on the angle-of-attack at which the vortex breakdown crosses the wing trailing edge (α_{BD-TE}) and the rate at which the breakdown progresses forward over the wing once α_{BD-TE} is reached. To increase strake efficiency, the designer wants to increase α_{BD-TE} and reduce the rate that the vortex breakdown moves forward. α_{BD-TE} is increased by increasing strake area and/or increasing strake slenderness. The Gothic strake planform was found to be better than the delta shape because the vortex core breaks up farther

into the wing pressure field, but strake shape is considered of secondary importance until nearing $C_{L_{max}}$. The primary or most significant geometric parameter appears to be the area of the strake. Lift created by the strake is primarily dependent upon the area of the strake-induced vortex, which is defined as the exposed strake area plus the wing platform area that falls within the projected strake exposed area A_{EFF} (Figure 1 and Survey Bibliography 3).

III. EXPERIMENTAL DATA

Data used for these analyses were obtained as part of a MICOM sponsored wind tunnel test conducted at AEDC on advanced interceptor missile designs. This applied research test program investigated missile designs which hopefully would exhibit improved performance for a typical ground-to-air interceptor. Three basic designs were considered, which are modifications of a typical body-tail configuration with tail controls. The three designs considered (1) planar folding wing, (2) folding wrap-around wing, and (3) added wing strakes. Only the wing strake data is analyzed here.

A. Apparatus and Test

This test was conducted in the AEDC VKF-A facility. Tunnel A is a continuous flow, closed loop wind tunnel capable of Mach numbers from 1.5 to 5.5. The test section is 40 by 40 inches. Angles-of-attack for this test ranged from -4 to $+20$, and control deflections were 0, -5 , -10 , and -15 for certain configurations; however, the strake runs were made with zero control deflection only and Mach 2.0 only. Table 1 presents the nominal test conditions.

B. Models and Data

An existing wind tunnel model was modified for these tests. Midsection wings and strakes were added to a basic body-tail configuration, as depicted in Figure 2. Geometric dimensions for the basic body-tail configurations are shown in Figure 3. Strake geometry and dimensions are shown in Figure 4.

Two geometric parameters were used in designing strakes for these tests: (1) the ratio of strake area to wing area and (2) the strake leading edge sweep-back angle. These two parameters are illustrated in Figure 5. Strake S_1 was not tested. Complete geometry of the body, strakes, wings, and

tail fins are tabulated in Tables 2 through 5. Nomenclature used for model components are presented in Table 6. The analysis in this report is concerned only with W_1 (straight wing) and strakes S_1 and S_2 in conjunction with the basic body-tail (B₁T₁).

Six-component main balance and three-component fin balance data were taken. Since differences between runs are of primary importance to this analysis, a thorough review of tunnel flow angularity and model aero bias was performed. It was concluded that flow angularity was small, as illustrated in Figures 6 and 7, and thus any non-zero stability coefficients at zero angle-of-attack would be considered as an aero bias. Since the wind tunnel model is intended to be symmetrical, any identifiable aero bias was shifted out of the coefficient data.

IV. RESULTS AND DISCUSSION

The effect of strakes on wing lift, tail lift, hinge moment, root bending moment, and body-wing-tail stability is examined. Six-component main balance data is used for the wing and body-wing-tail study, and three-component fin balance data is used for fin-alone study. Body buildup runs were made to enable component analysis. Any bias in the coefficient data was shifted to zero, assuming no flow angularity. Flow angularity was examined, as illustrated in Figures 6 and 7, and found to be insignificant.

A. Wings

The effect of strakes on wing plus wing-body interference lift is illustrated in Figures 8, 9, and 10. During the wind tunnel test, runs were made with body-alone and body-wing as well as body-wing-strake. Body-alone data is subtracted from body-wing and body-wing-strake data to determine the strake effect on wings. These data indicate that the strakes tested do not significantly influence the basic wing lift for angles-of-attack up to 20° . Perhaps the strake effect would be more pronounced near the stall point; however, test section restrictions limited the maximum angle-of-attack for this test. Roll angle effects on strakes are also insignificant, as illustrated in Figure 9. The ratio of wing lift with strakes to that without strakes (Figure 10) gives a better picture of the strake effect. It is surprising to find that the percent increase in wing-strake lift is approximately the same for both strakes (S_1 and S_2) near zero angle-of-attack. Strake

S_2 has twice the area of S_1 , but it does not give twice the increase in lift. At higher angles-of-attack (10° to 20°), S_2 , the larger strake, does yield approximately twice the effect of strake S_1 . The same holds true for both 0° and 45° roll angles. Another observation from Figure 10 is that the strake effect is greatest near zero angle-of-attack (about 6 to 7 percent) and reduces to about half that at 20° . This phenomenon seems contrary to the expected strake effect. Again, it should be remembered that the configuration and test conditions here are thin-wing missile type shapes at Mach 2.0 and might not be expected to yield the same results as airplane configurations at subsonic and transonic speeds.

B. Tail Fins

The effect of strakes on tail fin forces and moments is illustrated in Figures 11 through 15. Three-component fin balances were used to measure fin-alone loads plus upwash effects from the body to the fin. Runs were made with body-wing-tail and body-wing-strake-tail to isolate the effect of strakes on tail fins. The strake effect on tails is in the form of a changed downwash flow field from the wing to the tails. If the wing lift is increased, then a stronger downwash field exists, which results in reduced tail fin stabilizing effectiveness. It should be remembered that these test were made with in-line wings and tails.

Fin surface alignment is illustrated in Figure 11. As observed, fins 1 and 3 measure practically no load and fins 2 and 4 measure practically the same

load, indicating good model and component alignments. Consequently, when analyzing $\phi = 0^\circ$ data, only fin 2 or 4 data need be used. For $\phi = 45^\circ$ analysis, fins 1 and 2 will be used.

As can be observed in Figures 12, 13, and 14, the effect of strakes on tail fins is quite small for the conditions tested. The same is generally true for $\phi = 45^\circ$ as shown in Figure 15. These results indicate that the vorticity or downwash field from the wings to the tails is not changed significantly with added wing strakes. This is not surprising in light of the wing-strake analysis.

C. Total Configuration

Only strake S_2 was tested with the full configuration, due to limited tunnel time. Strake S_2 was selected, as opposed to S_1 or S_3 , because it was expected to give the greatest change in stability characteristics. The results are shown in Figures 16 through 18. Basically, the strakes have a small effect at $\phi = 0^\circ$ or 45° for the conditions tested. As with the wing-alone results, strake effects on total configuration are more pronounced at small angles-of-attack and decrease significantly up to 20° . The effect on Lift/Drag ratio (L/D) is also small, as shown in Figure 19. A very slight increase in L/D is obtained in the 4° through 10° angle-of-attack range, but not significant enough to warrant the increased weight. Figure 20 presents the L/D at Mach numbers 2, 3, and 4, without strakes. It is expected that the strake effects will be quantitatively the same throughout the Mach 2 to 4 range for the configurations tested.

V. CONCLUSIONS

1. The addition of forebody strakes to a missile type body-wing-tail configuration produces only a slight increase in wing lift (less than 5%) at Mach 2.0 and angles-of-attack up to 20° , for the configurations tested.
2. Tail fin loading is practically unaffected by the addition of strakes for the shapes and conditions tested.
3. Lift/ Drag ratios show no significant improvement in missile performance, due to added strakes, at Mach 2.0.
4. Body roll angle does not change the strake effect appreciably.

TABLE 1. NOMINAL TEST CONDITIONS

M	PT, psia	TT, °R	Q, psia	P, psia	RE/ft x 10⁻⁶
2.0	10.3	560	3.7	1.32	2.5
3.0	16.3	545	2.8	0.44	2.5
4.0	30.1	580	2.2	0.20	2.5

TABLE 2. BODY GEOMETRY (B₁)

Nose Bluntness	0.020
Overall Length	48.832
Nose Length (Ogive-Conical Frustrum)	12.573
Reference Diameter	3.75
Reference Area (in. ²)	11.045
Moment Reference Center	0.0
Tail Fin Pivot Station	45.705
Boat-tail Length	2.110
Base Diameter	3.445
Wing L.E. Station	24.375

NOTES: All stations and lengths are relative to ogive theoretical tip (0.020 forward of actual nose).

All dimensions in inches unless otherwise noted.

TABLE 3. STRAKE GEOMETRY (S_i)

	S ₁	S ₂	S ₃
Exposed Semi-Span	1.4824	1.336	0.9446
Root Chord	2.028	4.5	3.1819
Tip Chord	0	0	0
Area, Single Panel Exposed (in. ²)	1.503	3.006	1.503
L.E. Sweepback Angle (deg)	60	75	75
T.E. Sweepback Angle (deg)	20	20	20
Station of L.E. Root Chord	22.347	19.875	21.193
Aspect Ratio	2.924	1.188	1.188
Taper Ratio	0	0	0
Strake Thickness (in.)	0.100	0.100	0.100

NOTE: All dimensions in inches unless otherwise noted.

TABLE 4. WING GEOMETRY (W_i)

	W ₁	W ₂ Projected
Exposed Semi-Span	4.5	2.794
Root Chord	7.5	7.5
Tip Chord	5.862	6.483
Area, Single Panel Exposed (in. ²)	30.065	19.572
Leading Edge Sweepback Angle (deg)	20	20
Trailing Edge Sweepback Angle (deg)	0	0
Station of Leading Edge Root Chord	24.375	24.375
Aspect Ratio	1.347	0.80
Taper Ratio	0.782	0.864
Root Chord Thickness Ratio	0.050	0.040
Tip Chord Thickness Ratio	0.050	0.040

NOTE: All dimensions in inches unless otherwise noted.

TABLE 5. TAIL GEOMETRY (T₁)

Exposed Semi-Span	2.079
Root Chord	6.791
Exposed Semi-Span (Includes 0.036-in. Gap)	2.115
Root Chord (Includes 0.036-in. Gap Extension to Surface)	6.861
Tip Chord	2.716
Area, Single Panel Exposed (in. ²)	9.883
Leading Edge Sweepback Angle (deg)	62.964
Trailing Edge Sweepback Angle (deg)	0
Station of L.E. Root Chord (Theoretical Extension to Surface)	41.704
Taper Ratio	0.40
Root Chord Thickness Ratio	0.069
Tip Chord Thickness Ratio	0.076
Station of Pivot Point	45.705
Reference Area	11.045
Reference Length	3.75
Reference Hinge Line	1/4 MAC
Aspect Ratio	0.875

NOTE: All dimensions in inches unless otherwise noted.

TABLE 6. CONFIGURATION NOMENCLATURE

Body Alone (B₁)

Tail Fins (T₁)

Straight Wing (W₁)

Curved Wing (W₂)

Simulated Straight Wing Folded (F₁)

Simulated Curved Wing Folded (F₂)

Strakes 1, 2 or 3 (S_x)

REFERENCES

1. Killough, T. L. and W.D. Washington, "Pretest Report for an Improved Army Interceptor Design." MICOM Internal Technical Note T-79-16, April 1979.
2. Chafin, J. M. and J. C. Sung, "User's Guide for Advanced Interceptor Design (ADVINT) Aerodynamic Data Base." New Technology, Inc., TR1020, September 1979.
3. Best, J. T., Jr., "Static Force Test on an Improved Army Interceptor Design at Mach Numbers 2.0 to 4.0," AEDC-TSR-79-V41, August 1979.

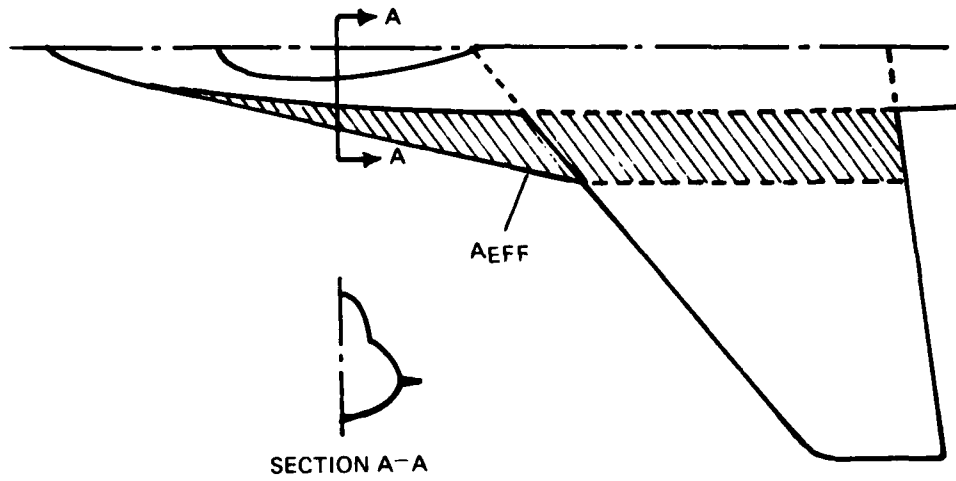


Figure 1. Definition of effective strake area for a simple wing-body configuration.

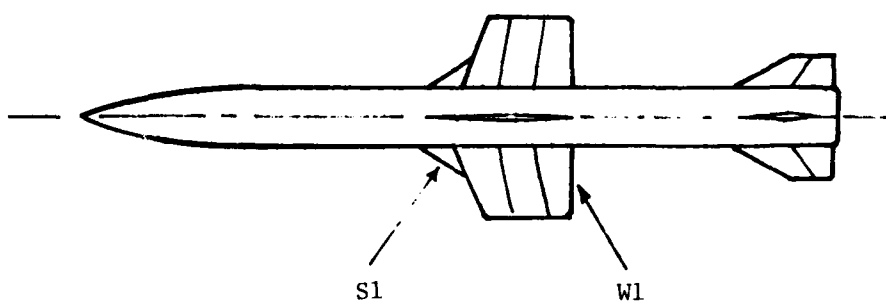
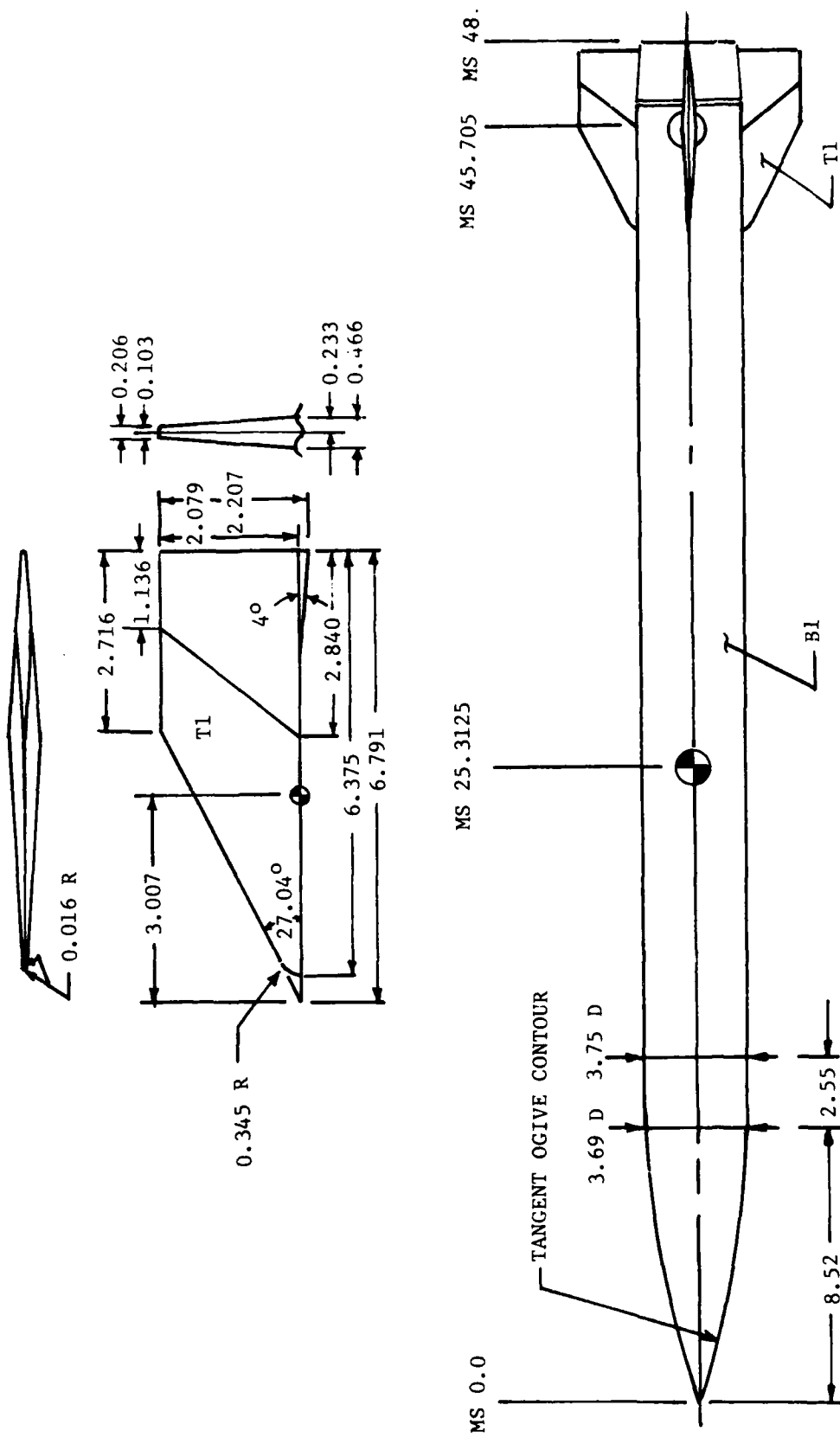


Figure 2. Typical Configuration.



● MOMENT REFERENCE POINT
 ALL DIMENSIONS IN INCHES UNLESS
 OTHERWISE STATED

Figure 3. Body-tail details.

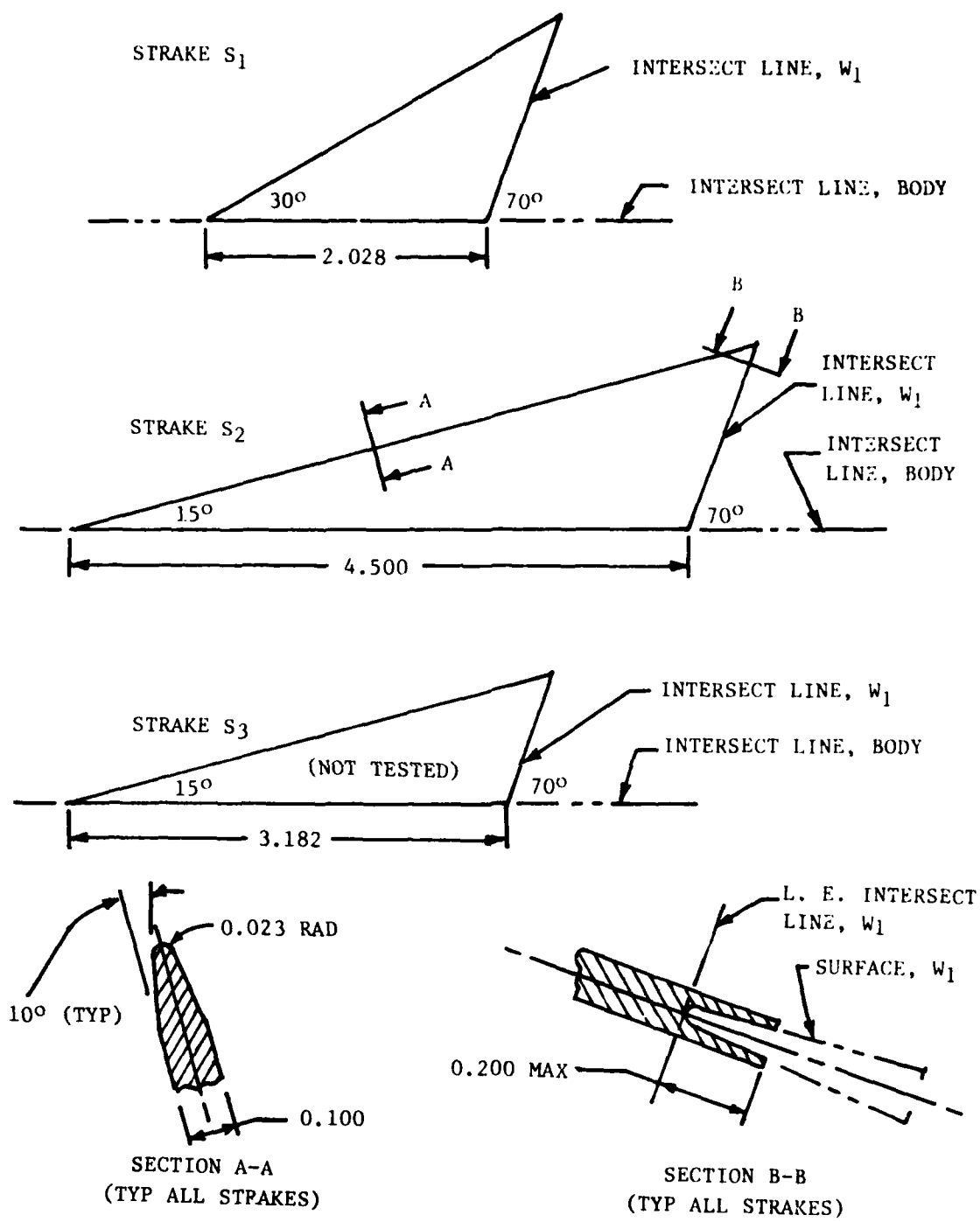
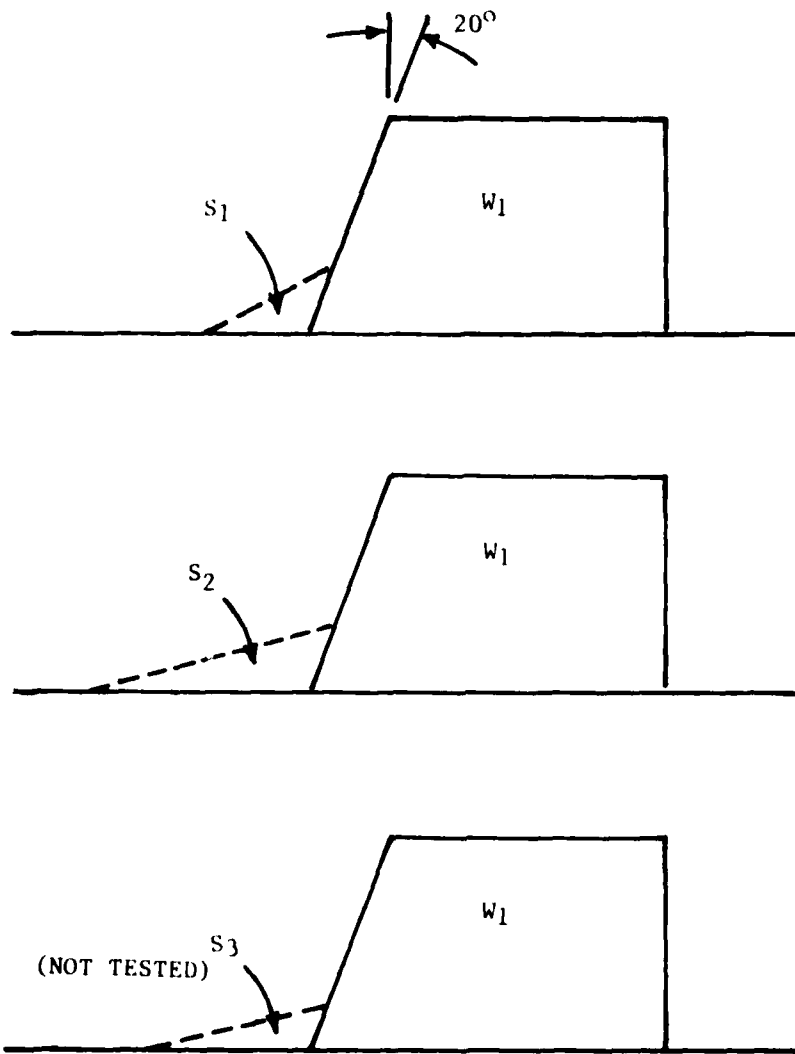


Figure 4. Strake dimensions (inches).



Strake	Area Ratio to Wing (%)	Span Ratio to Wing (%)	Leading Edge Sweepback Angle (deg)	Root Chord Ratio Wing (%)
1	5	32.9	60	27.0
2	10	29.7	75	60.0
3	5	21.0	75	42.4

Figure 5. Strake size relative to wing (W_1)

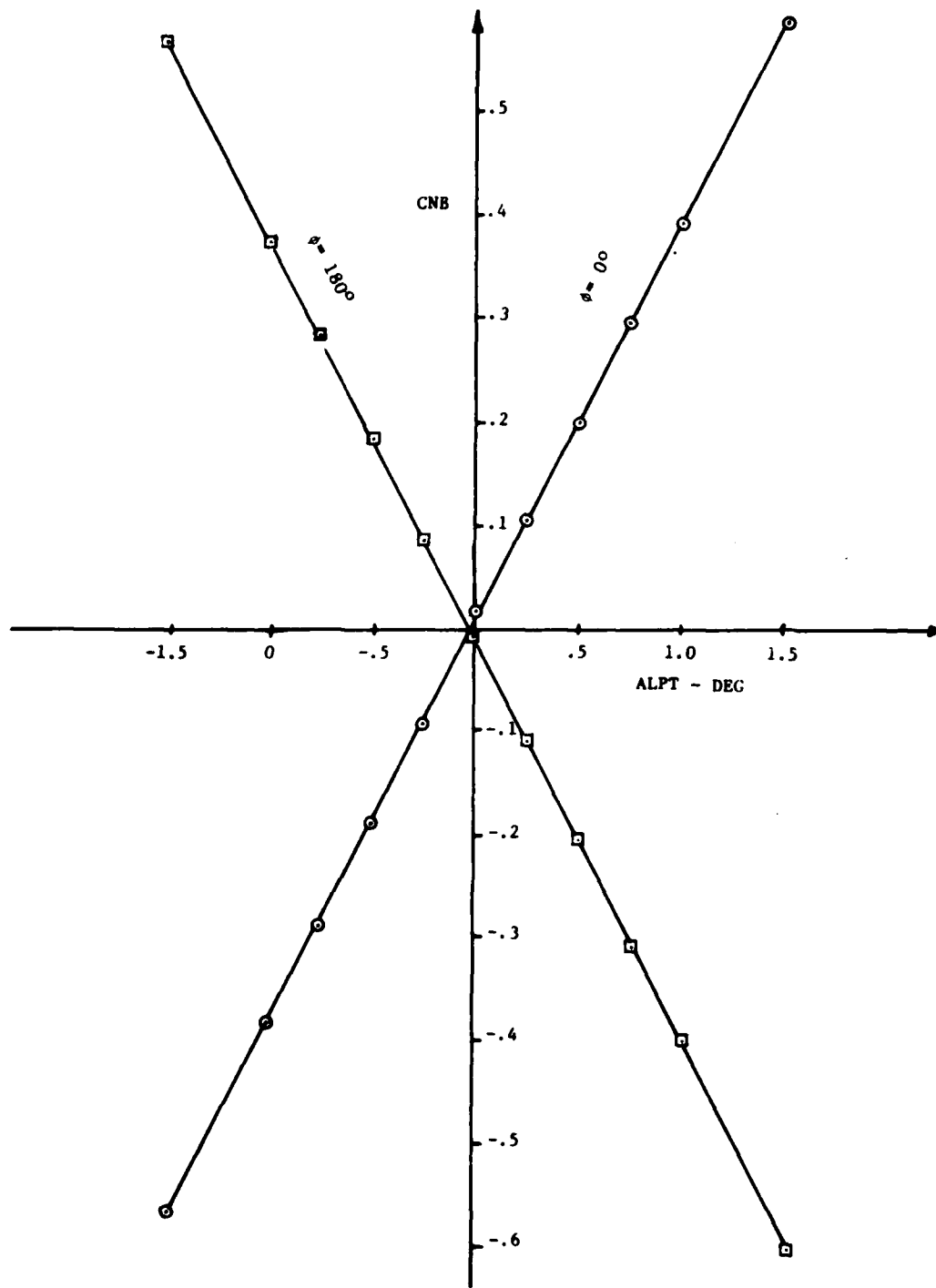


Figure 6. Flow angularity ($M_\infty = 2$).

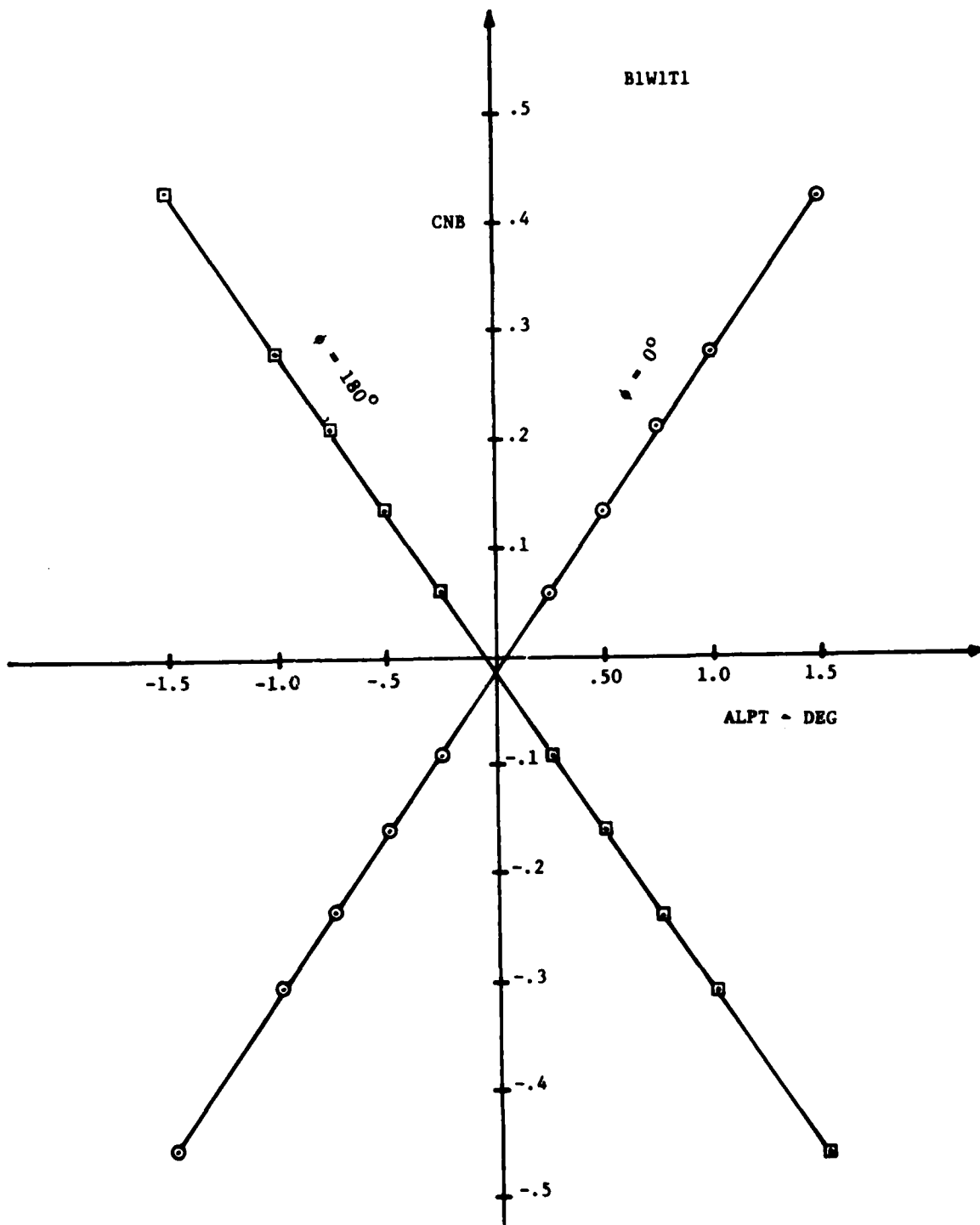


Figure 7. Flow angularity ($M_\infty = 3$).

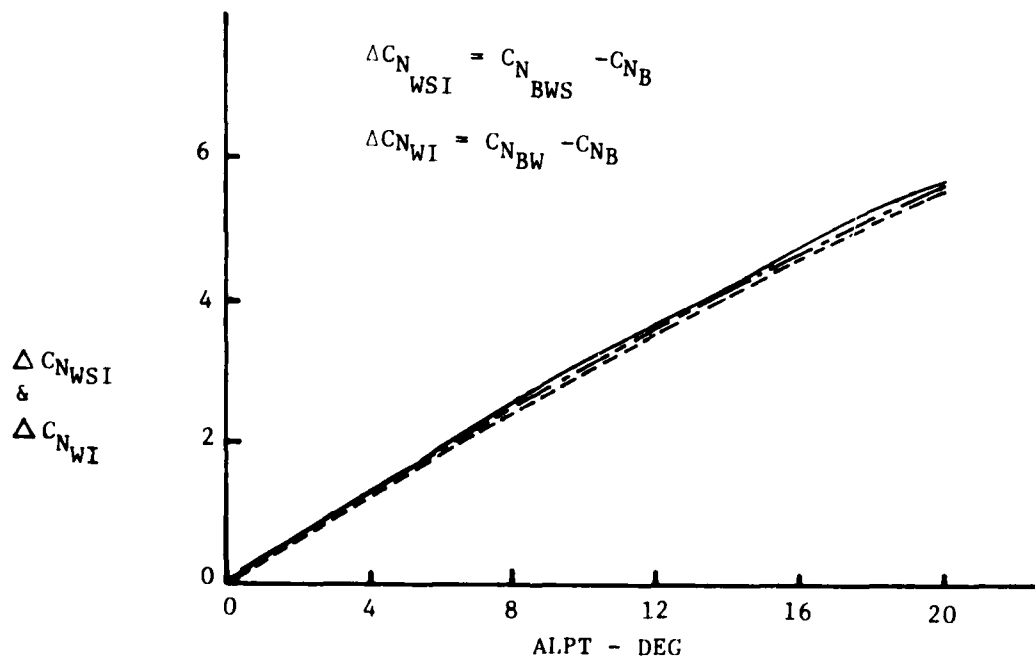
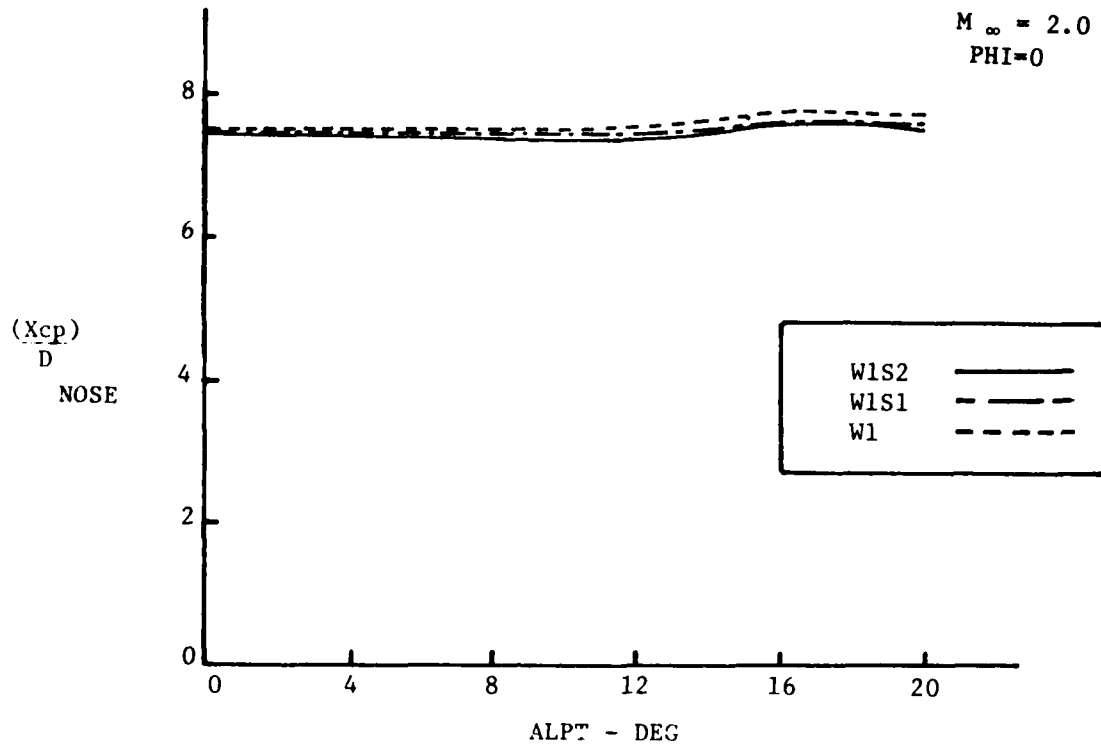


Figure 8. Effect of strakes on wing plus wing-body interference ($\phi = 0^\circ$).

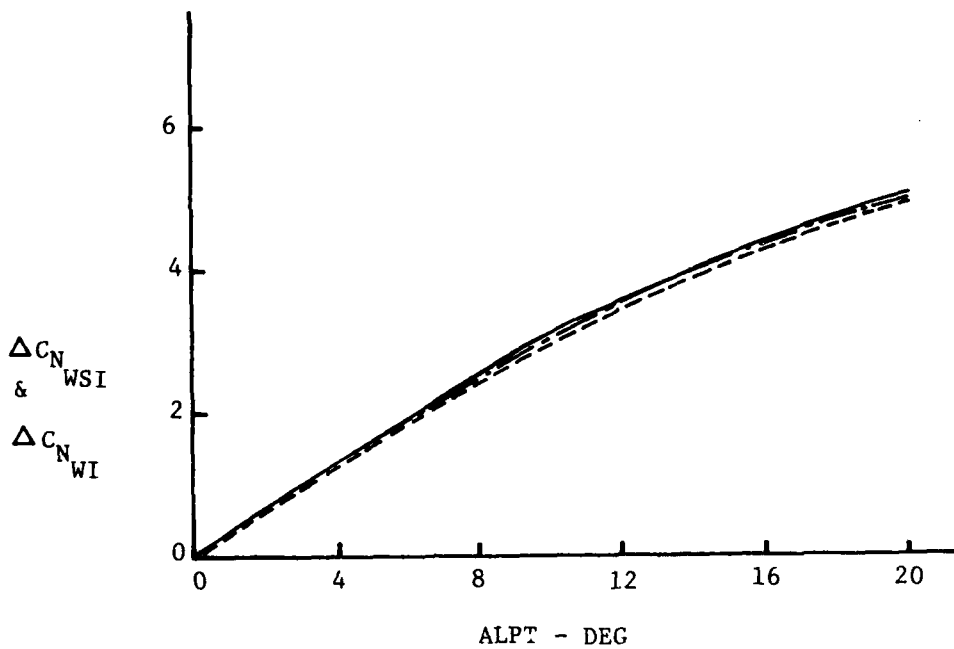
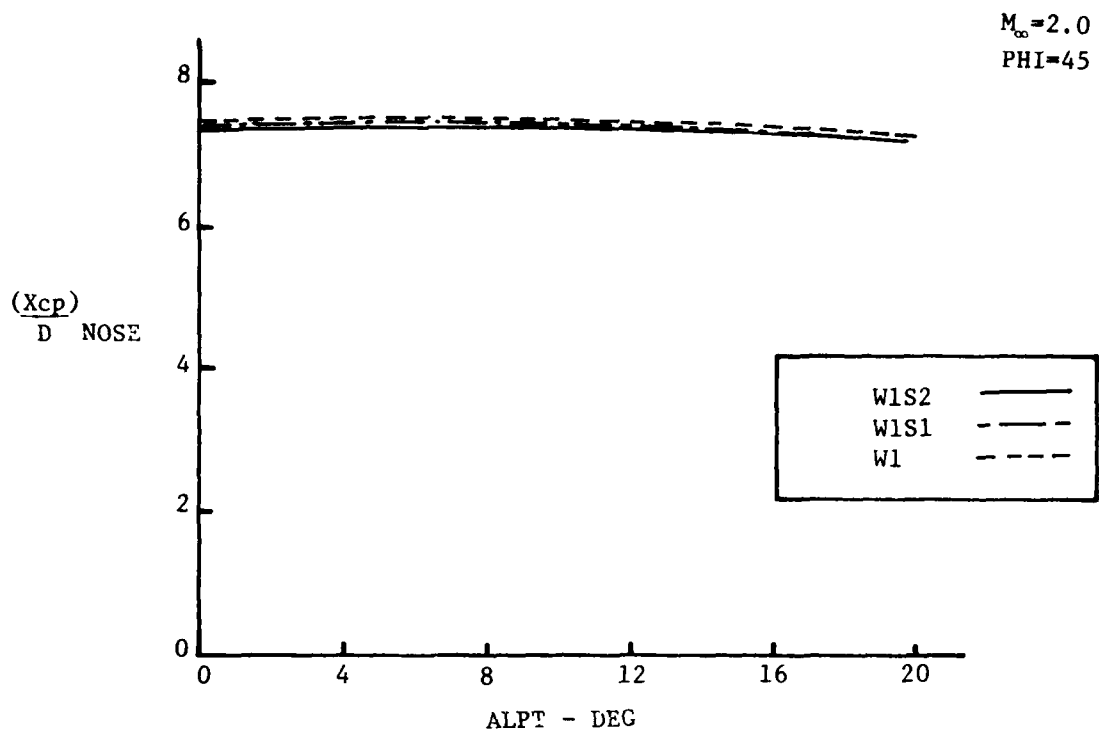


Figure 9. Effect of strakes on wing plus wing-body interference ($\phi = 45^\circ$).

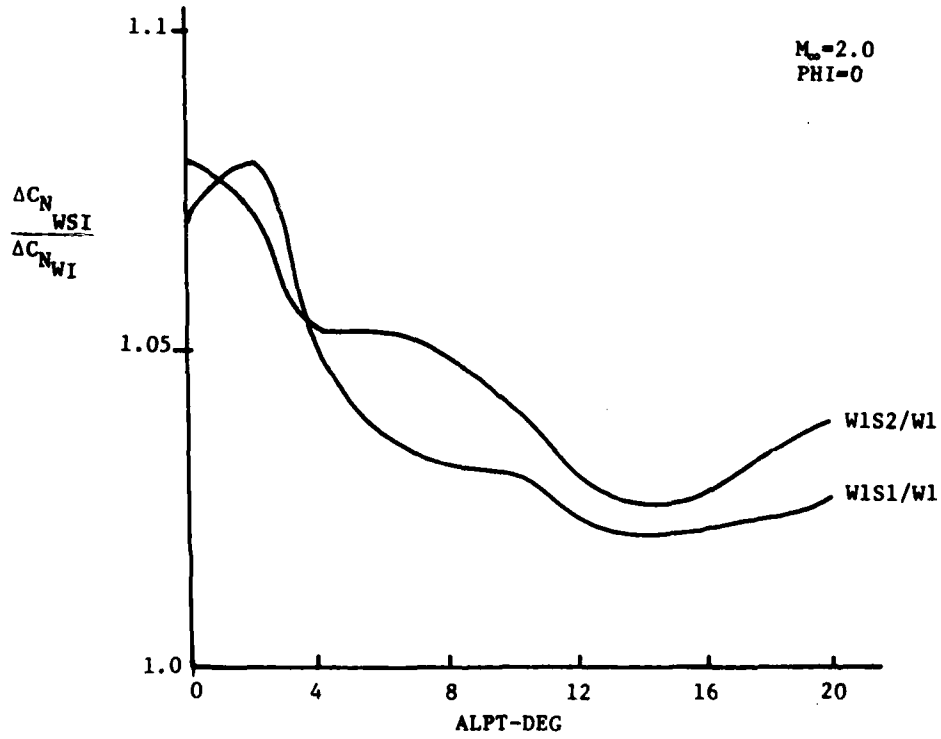
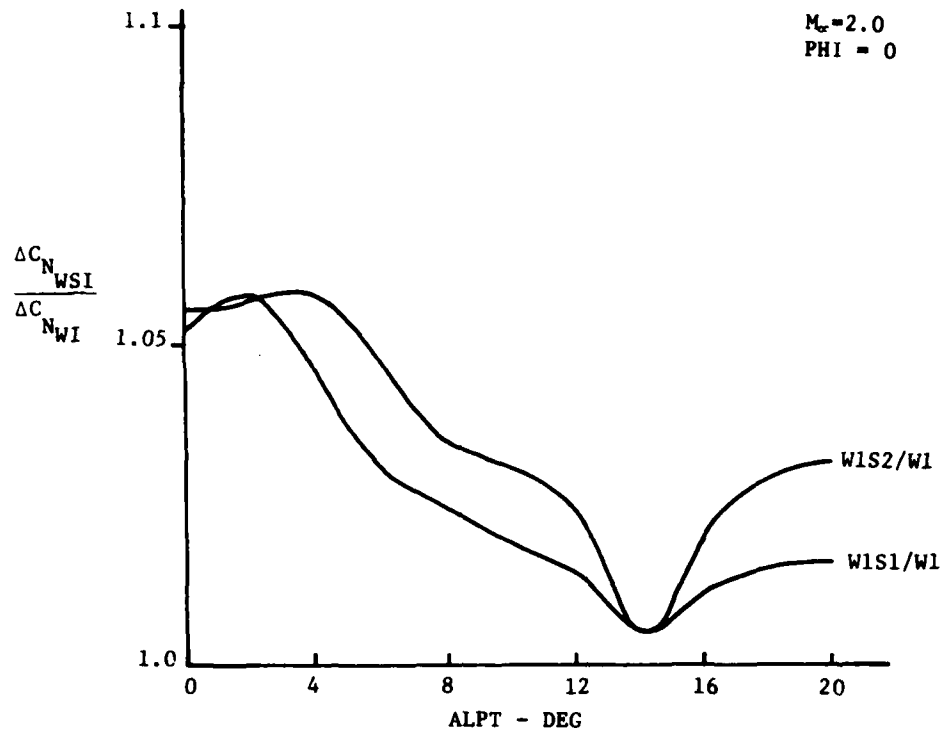


Figure 10. Normal force ratio (wing with strake/wing without strake).

B1W1S2T1

$M_\infty = 2.0$
 $\text{PHI} = 0$

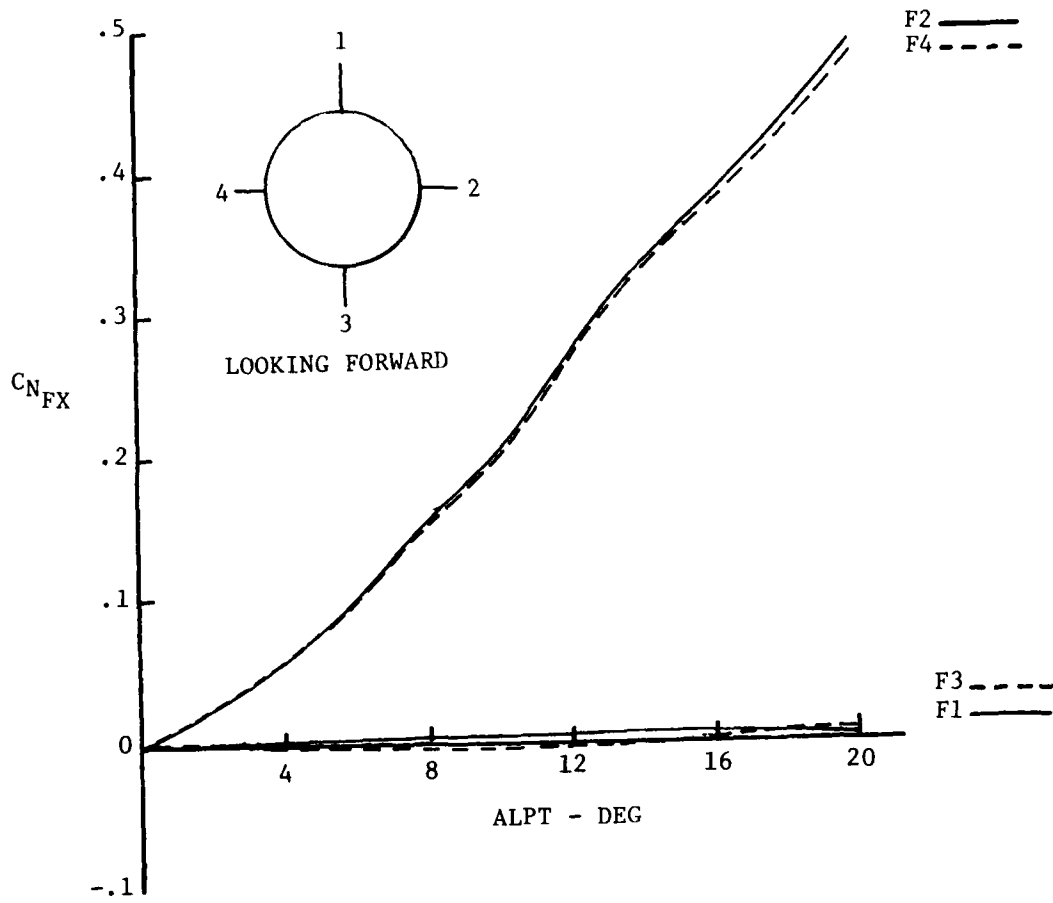


Figure 11. Fin normal force (all fins).

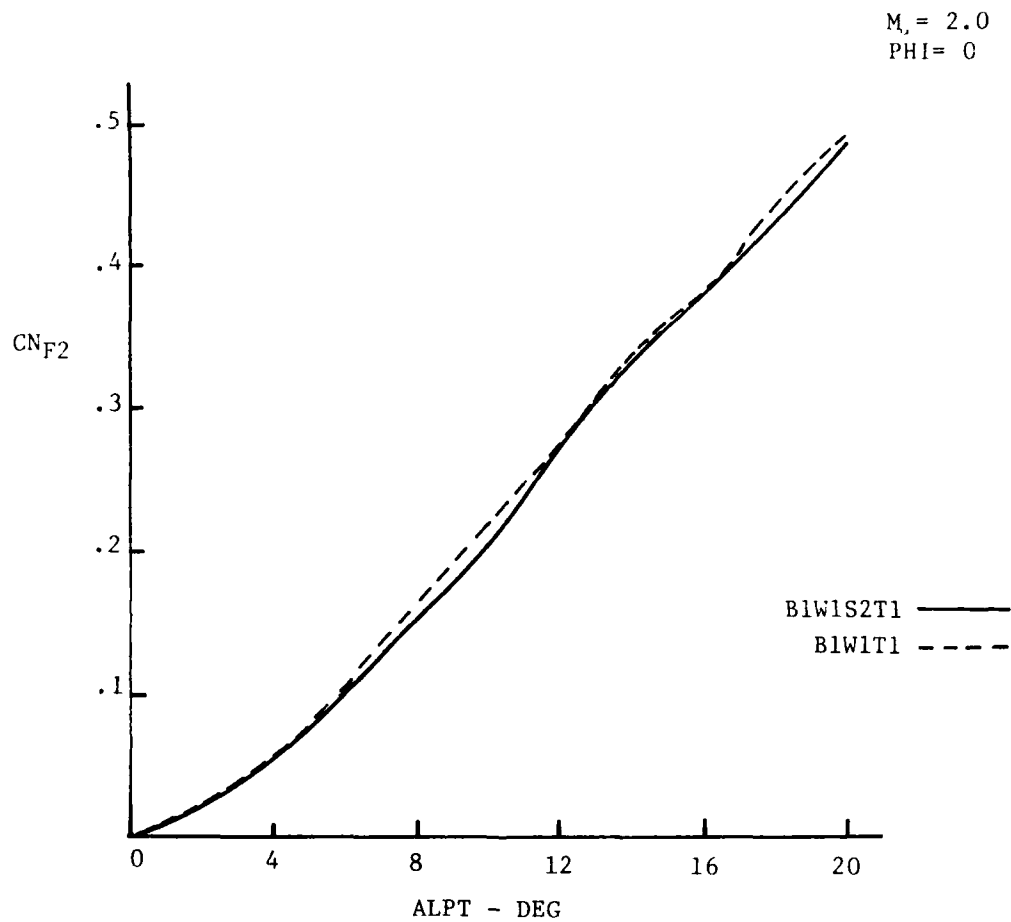


Figure 12. Effect of strake S_2 on fin normal force.

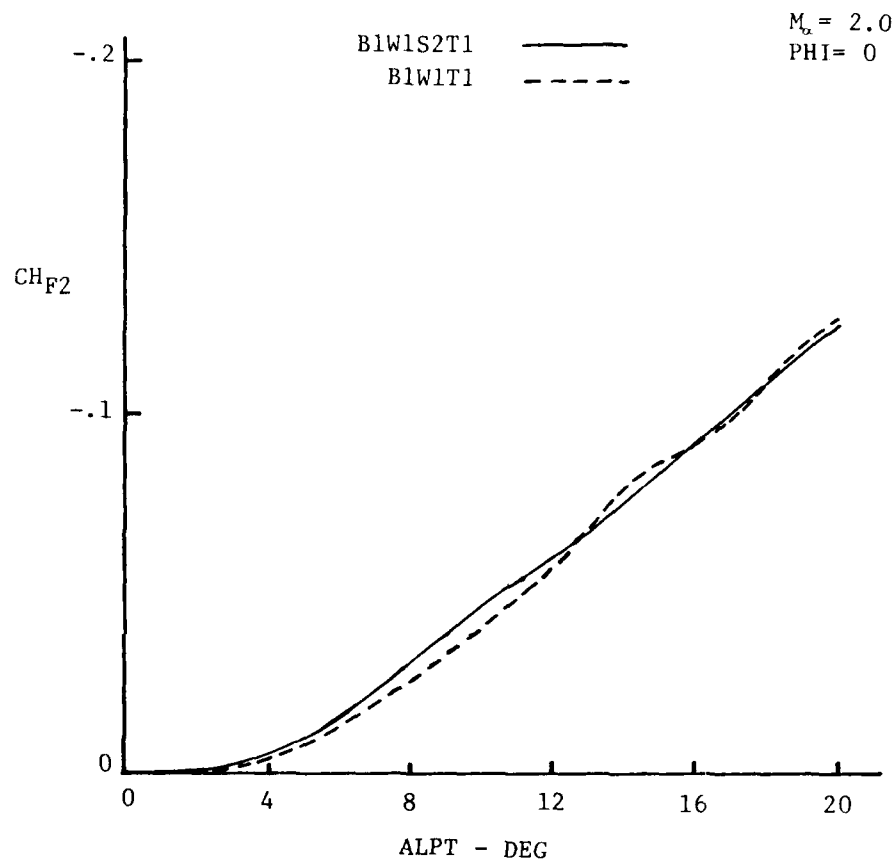


Figure 13. Effect of strake S_2 on fin hinge moment.

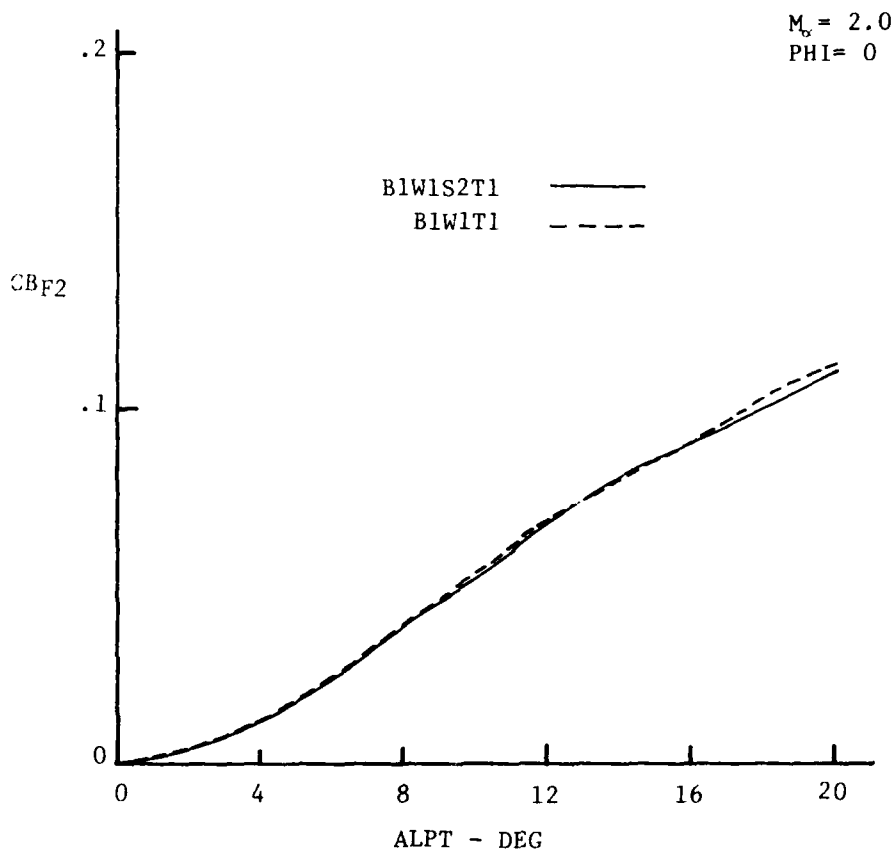


Figure 14. Effect of strake S_2 on fin root bending moment.

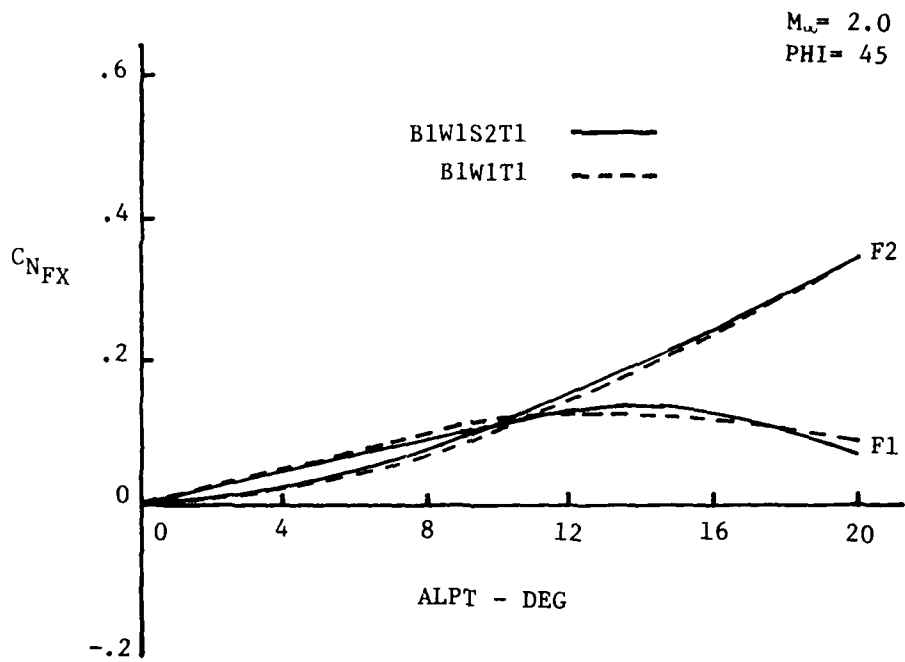


Figure 15. Strake S₂ effect on fin normal force at $\phi = 45^\circ$.

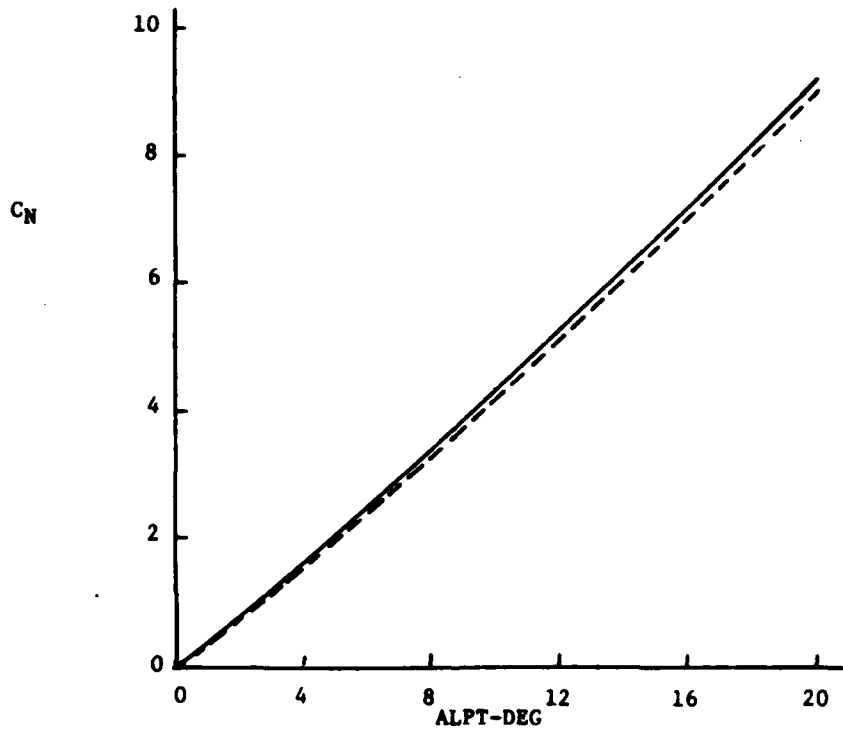
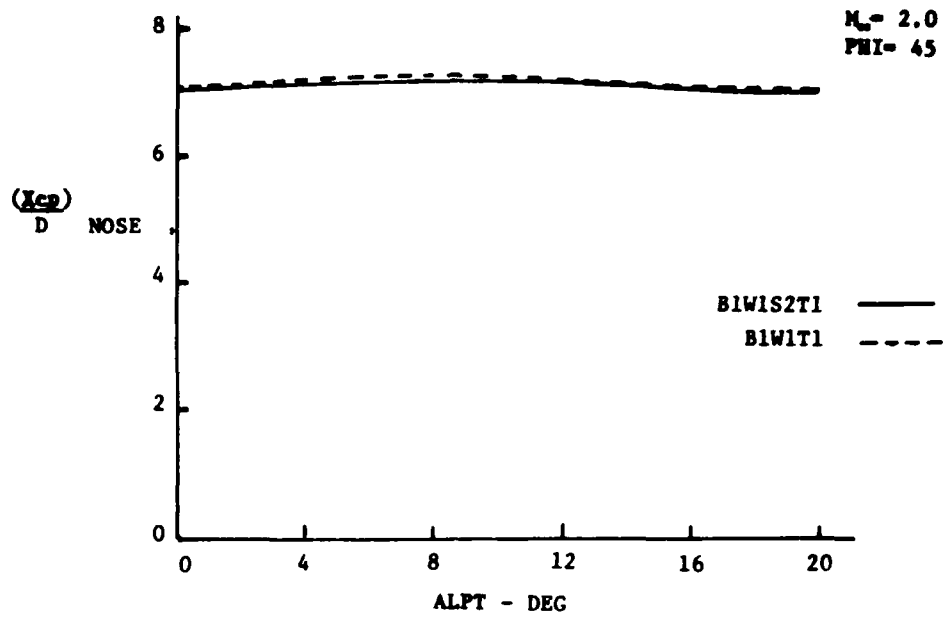


Figure 16. Effect of strake S_2 on total configuration stability ($\phi = 0^\circ$).

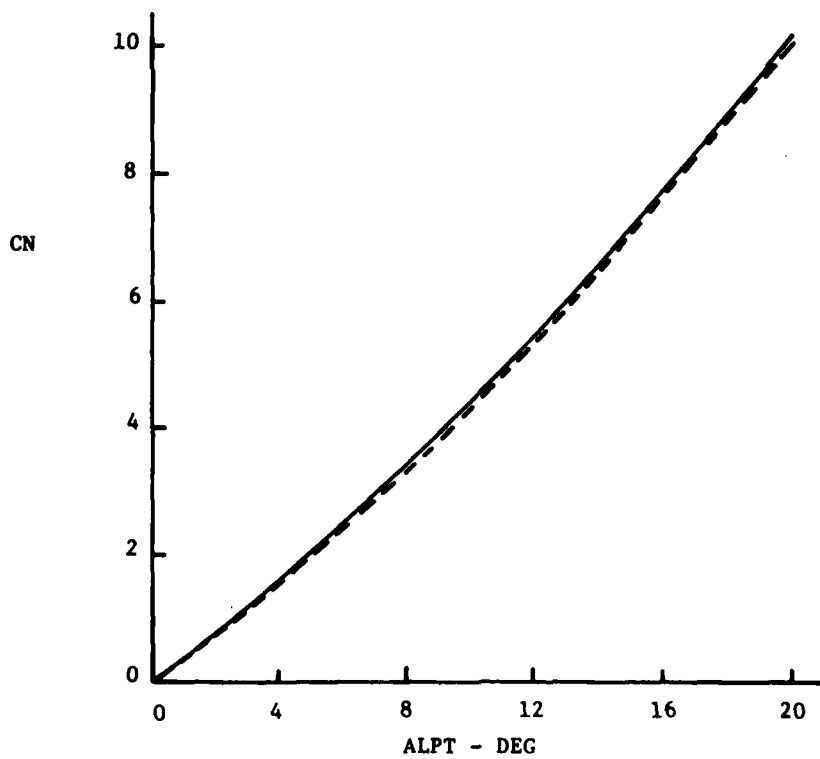
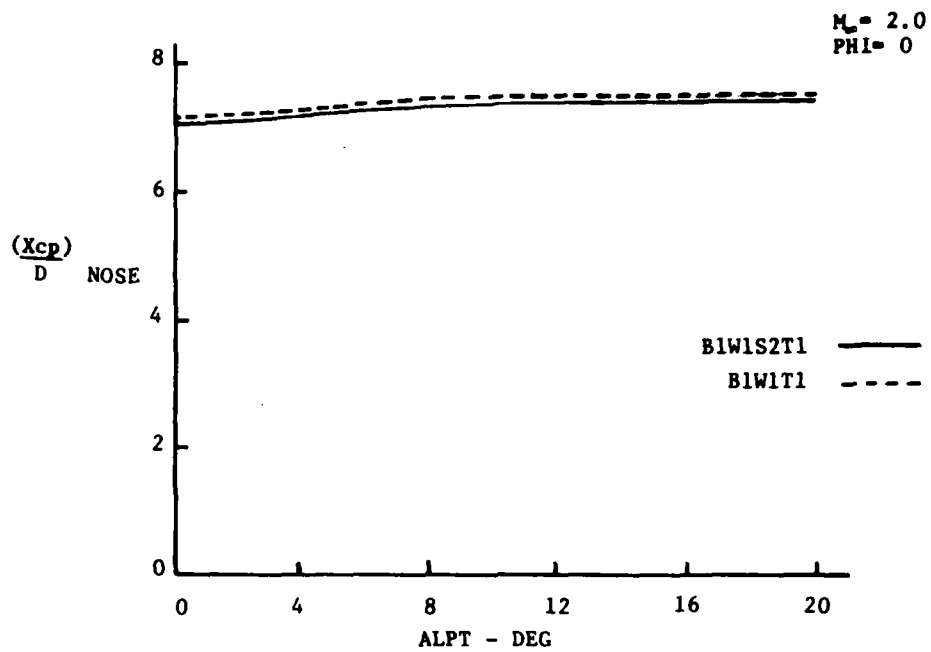


Figure 17. Effect of strake S_2 on total configuration stability ($\phi = 45^\circ$).

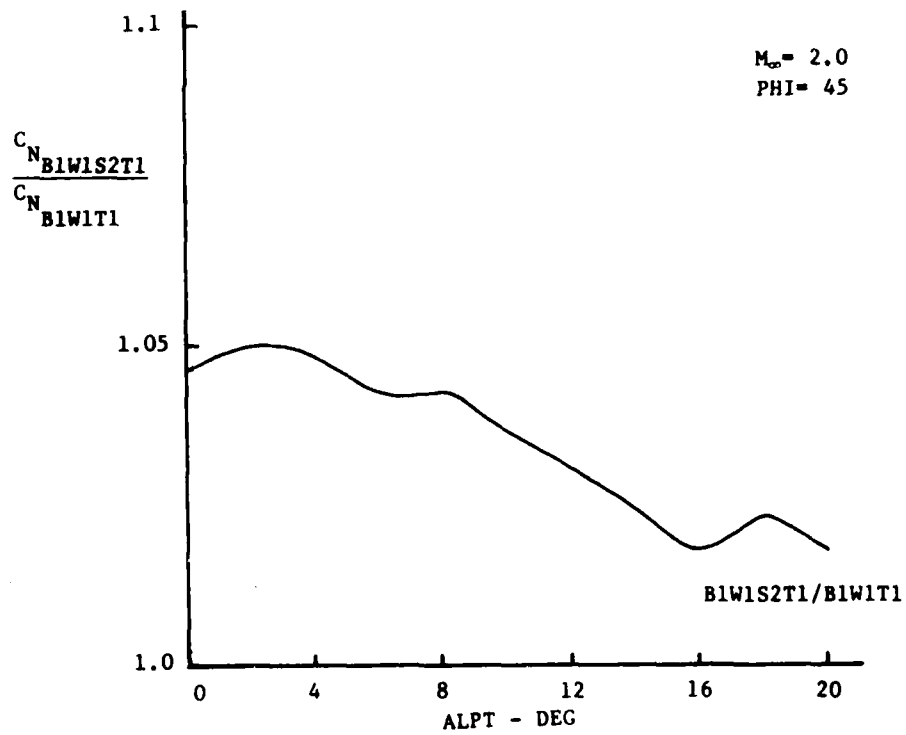
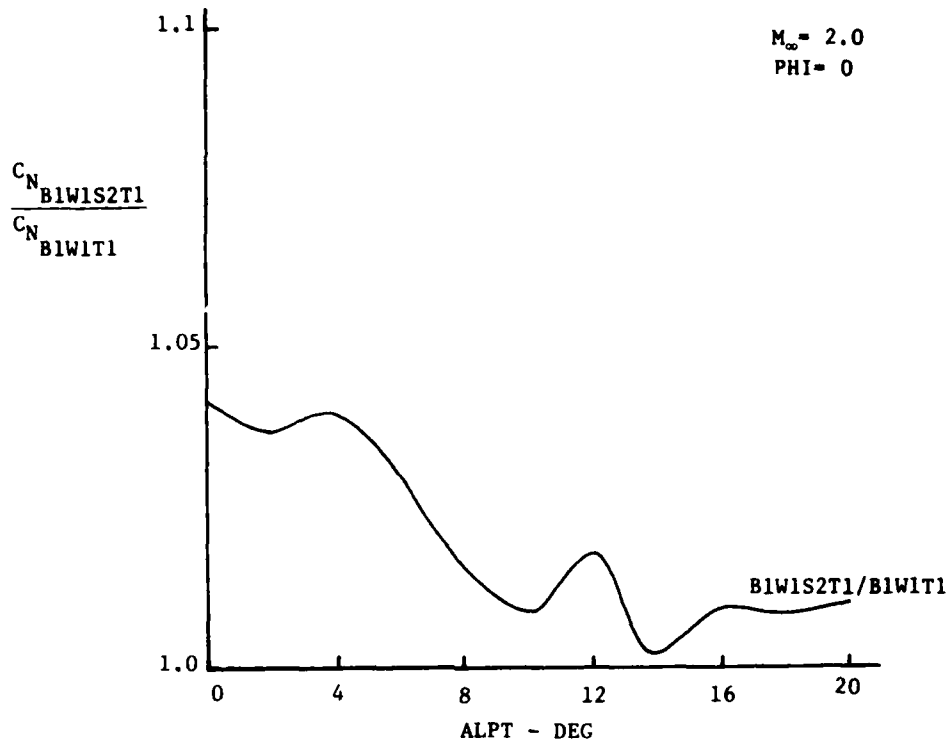


Figure 18. Ratio of total normal force with and without strakes.

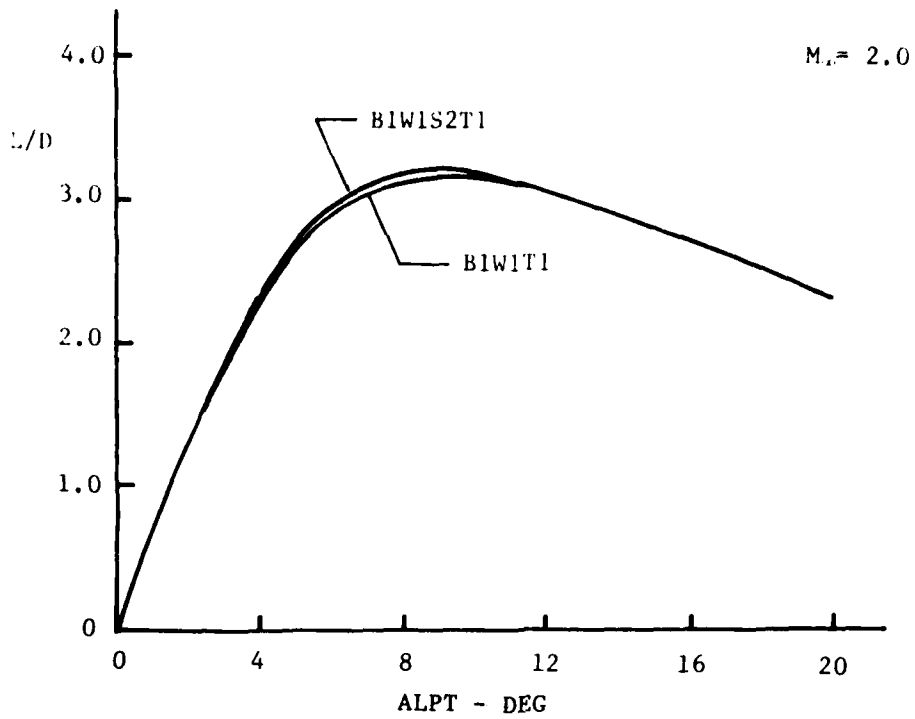


Figure 19. Effect of strake S_2 on lift/drag ratio.

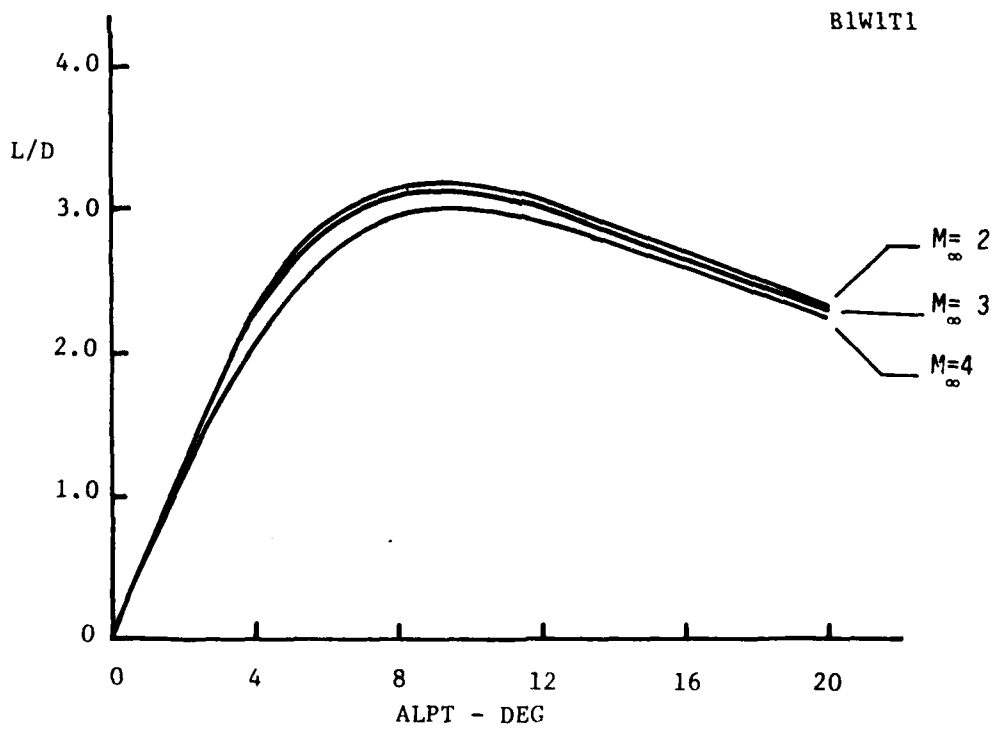


Figure 20. Effect of Mach number on lift/drag ratio (no strake).

SURVEY BIBLIOGRAPHY

1. Brohez, G., B. Movassaghie, W. Stahl, "Aerodynamic Characteristics of a Missile Configuration Featuring a Wing with Strakes," N78-17022, August 1977.
2. Stahl, W., "On the Effect of a Strake on the Flow Field of a Delta Wing ($\lambda=2$) at Near-Sonic Velocities," DGLR Paper No. 72-125, July 1975.
3. Anderson, C. A., C. W. Smith, "Design Guidelines for the Application of Forebody and Nose Strakes to a Fighter Aircraft Based on F-16 Wind Tunnel Testing Experience," AGARD-CP-247 Paper No. 5, January 1979.
4. Lamar, J. E., "Strake-Wing Analysis and Design," AIAA Paper 78-1201, July 1978.
5. Luckring, J. M., "Theoretical and Experimental Aerodynamics of Strake-Wing Interactions up to High Angles-of-Attack," AIAA Paper 78-1202, July 1978.
6. Liu, M. J., et al., "Flow Patterns and Aerodynamic Characteristics of Wing Strake," AIAA Paper 79-1877, August 1979.
7. Frink, N. T., and J. E. Lamar, "An Analysis of Strake Vortex Breakdown Characteristics in Relation to Design Features," AIAA Paper 80-0326, January 1980.
8. Bernstein, D., L. Bodin, and J. Soddarth, "Analysis Report of Transonic and Supersonic Wind Tunnel Tests for AGM-69A (.182 scale)," Wright-Patterson Air Force Base, ASD-TR-66-56, 1965.
9. Moss, G., "Some UK Research Studies of the Use of Wing-Body Strakes on Combat Aircraft Configurations at High Angles of Attack," AGARD-CP-247 Paper No. 4, January 1979.
10. Fiddes, S. P. and J. H. B. Smith, "Strake-Induced Separation from the Leading Edges of Wings of Moderate Sweep," AGARD-CP-247 Paper No. 7, January 1979.
11. Laschka, B., J. P. Ledy, P. H. Poisson-Quinton, and W. Staudacher, "Aerodynamic Characteristics of a Fighter-Type Configuration During and Beyond Stall," AGARD-CP-247 Paper No. 8, January 1979.
12. Akcay, M., B. E. Richards, W. Stahl, and A. Zarghami, "Aerodynamic Characteristics of a Missile Featuring Wing with Strakes at High Angles of Attack," AGARD-CP-247 Paper No. 20, January 1979.
13. Lamar, J. E. and J. M. Luckring, "Recent Theoretical Developments and Experimental Studies Pertinent to Vortex Flow Aerodynamics with a View towards Design (Review Paper)," AGARD-CP-237 Paper No. 24, January 1979.

NONMENCLATURE

A	Reference area, body cross section
A_{DV}	Area affected by strake-induced vortex
AF	Fin reference area, body cross section
ALPT	Total angle-of-attack, missile axes-DEG
CBF2	Fin 2 bending-moment coefficient, bending moment, $Q AF D$
CHF2	Fin 2 hinge-moment coefficient, hinge moment $Q AF D$
$C_{l,max}$	Maximum lift coefficient
CN	Normal force coefficient, missile axes, normal force/ $Q A$
CNB	Normal force coefficient, body axes, normal force/ $Q A$
CNFX	Fin normal force coefficient for fin X, fin axes, normal force/ $Q AF$
ΔCN	Incremental normal force coefficient
D	Reference diameter, cylinder
L/D	Lift/drag ratio
M_{∞}	Free-stream Mach number
P	Free-stream static pressure, psia
PHI, θ	Roll angle, deg
PT	Tunnel stilling chamber pressure, psia
Q	Free-stream dynamic pressure, psia
RE	Free-stream unit Reynolds number, ft^{-1}
TT	Tunnel stilling chamber temperature, °R
WI	Wing plus interference
WSI	Wing plus strake plus interference
XCP	Center-of-pressure location, from model nose
α_{BD-TE}	Angle-of-attack at which strake vortex breakdown crosses the wing trailing edge

DISTRIBUTION

Office of Naval Research 800 N. Quincy St. Arlington, VA 22217 ONR 211 ONR 430B	1 1	NASA AMES Research Center Moffett Field, CA 94035 Dr. G. Chapman Mr. J. Malcolm	1 1
Defense Technical Information Center Bldg. 5 Cameron Station Alexandria, VA 22314	12	Wright Patterson Air Force Base Dayton, OH 45433 AFFDL EGC (Dr. G. Kurylovich)	1
Naval Air Systems Command Washington, DC 20361 AIR 320C (Mr. W. Volz)	1	Eglin Air Force Base Eglin, FL 32542 AFATL DIDL (Mr. D. C. Daniel)	1
Naval Surface Weapons Center White Oak Laboratory Silver Spring, MD 20910 Code WA-41 (Mr. F. J. Regan) (Dr. Leon Schudd)	1 1	Arnold Engineering Development Center Arnold AF Station, TN 37389 AFDC DYR (Mr. E. R. Thompson)	1
Naval Surface Weapons Center Dahlgren Laboratory Dahlgren, VA 22448 Code DK-21 (Dr. F. Moore)	1	Wright Patterson Air Force Base Dayton, OH 45433 AFFDL EGC (Mr. Calvin Dyer) AFFDL (Mr. Val Dahlem)	1 1
U. S. Naval Postgraduate School Monterey, CA 93940 Dept. of Aeronautics (Code 57)	1	Air Force Office of Scientific Research Bldg. 410 Bolling AFB, DC 20332 Aerospace Sciences (NA)	1
Naval Sea Systems Command Washington, DC 20362 SEA 0351 (Mr. L. Pasiuk)	1	Hughes Aircraft Corp. Missile Systems Division Canoga Park, CA 91304 Mr. J. B. Harrisberger	1
Naval Weapons Center China Lake, CA 93555 Code 3914 (Mr. W. H. Clark)	1	University of Notre Dame Aerospace and Mechanical Engineering P. O. Box 537 Notre Dame, IN 46556 Dr. R. Nelson	1
Pacific Missile Test Center Point Mugu, CA 93041 Code 1241 (Mr. K. A. Larsen) Dr. Lloyd Smith	1	Johns Hopkins University Applied Physics Lab. 8621 Georgia Avenue Silver Spring, MD 20910 Mr. L. E. Tisserand	1
David Taylor Naval Ship Research and Development Center Bethesda, MD 20084 Code 1606 (Dr. S. de los Santos)	1	Rockwell Missile Systems Div. 4300 East Fifth Avenue Columbus, OH 43216 Mr. Fred Hessman	1
NASA Langley Research Center Hampton, VA 23665 Mr. W. C. Sawyer M S 413 Mr. C. M. Jackson M S 406	1 1		

Martin Marietta P. O. Box 5837 Orlando, FL 32808 Mr. G. Aiello	1	Lockheed Missile & Space Co. P. O. Box 504 Sunnyvale, CA 94088 Dept. 81-10, Bldg. 154, (Dr. Lars E. Ericsson)	1
McDonnell Douglas Astronautics East P. O. Box 516 St. Louis, MO 63166 Mr. J. L. Bledsoe	1	NASA Langley Research Center Hampton, VA 23665 Miss Emma Jean Landrum, M/S 402	1
McDonnell Douglas Astronautics West 5301 Bolsa Avenue Huntington Beach, CA 92647	1	Nielsen Engineering & Research Inc. 510 Clyde Ave. Mountain View, CA 94043 Dr. Jack Nielsen	1
Sandia National Laboratories Albuquerque, N.M. 87185 Dr. William L. Oberkamp	1	US Army Materiel Systems Analysis Activity ATTN: DRXSY-MP Aberdeen Proving Ground, MD 21005	1
ARO Inc. PWT 4T Arnold AFS, TN 37389 Dr. T. Hsieh Dr. W. Baker	1 1	IIT Research Institute ATTN: GACIAC 10 West 35th Street Chicago, IL 60616	1
Aberdeen Proving Ground Ballistics Research Laboratory Aberdeen, MD 20015 Dr. Charlie H. Murphy	1	DRSMI-LP, Mr. Voigt -R -RDK, David Washington -RDK, Pam Alstott -RPR -RPT (Reference Copy) (Record Set)	1 1 15 5 3 1 1
Applied Sciences Division Large Caliber Laboratory Picatinny Arsenal, NJ 07801 Mr. Alfred A. Loeb	1		
AEDC DOTR Arnold AFS, TN 37389 A. F. Money	1		

